C h a p t e r   3

PHOTOACTIVATED TREATMENT USING VISIBLE LIGHT

This work has been done in collaboration with CJ Yu, Dennis Ko, and Muzhou Wang. Dr. CJ Yu synthesized PEGylated Eosin Y. Undergraduates Dennis Ko and Muzhou Wang assisted with spatial control and temporal control experiments respectively.

3.1 Introduction

Treatment of keratoconus and degenerative myopia have been proposed that aim to prevent tissue deformation by reinforcing the tissue, using crosslinking, which has been shown to increase tissue modulus and strength (Chapter 2). Wollensak, Seiler, Spoerl, and co-workers have developed a photoactivated crosslinking system as a potential treatment to arrest progression of keratoconus.[1-14] Through a series of laboratory and clinical studies, these investigators have demonstrated the efficacy of this treatment for keratoconus, and examined the possibility of using this treatment for degenerative myopia. A photosensitizing agent (riboflavin) is administered to the cornea then activated by excitation with ultraviolet light (UV-A), inducing crosslinking within the tissue. *In vitro*

study of UV-A irradiation after treatment with riboflavin showed an increase in modulus greater than 3 times for human corneal strips[8] and human sclera specimens.[20] *In vivo* experiments in a rabbit model showed that UV-A/riboflavin treatment of the cornea caused a 12% increase in collagen fiber diameter, an effect that may contribute to the increase in corneal modulus.[14] FDA clinical trials are currently underway to determine the safety of UV-A/riboflavin treatment for keratoconus.

Photoactivated crosslinking systems such as UV-A/riboflavin have advantages in temporal and spatial control over traditional crosslinking agents or reducing sugars. First, traditional crosslinkers begin to react as soon as they contact the tissue and create intermediary products that can continue reacting for minutes to days after removal of the excess reducing sugars. This effect is evident in the additional 50% increase of the shear modulus observed over the first 24 hours after rinsing excess glyceraldehyde from the sclera (Figure 2.16). Ideally, a photoactivatable solution could be delivered to an area and then allowed to diffuse into tissue before activation. Then upon activation, crosslinking would commence. After irradiation, no further modification would occur, giving the ability to precisely control the degree of crosslinking. Second, traditional crosslinking is mediated by small molecules that spread quickly by diffusion—both into the intended tissue and surrounding tissues. In the eye, there is the potential that crosslinking agents will be swept away in tears and in circulation, and there is a potential hazard that agents like GA will continue creating crosslinks as they move through the body. This poses a danger in the eye where crosslinking in sensitive areas, such as the retina, should be avoided. Photoactivated crosslinking can be localized to the intended area by selective irradiation.

While crosslinking with UV-A/Riboflavin does provide greater control than crosslinking with glyceraldehyde or other reducing sugars, the UV irradiation lasts 30 minutes and has potential toxicity, especially when combined with photoinitiator activation. Indeed, toxic effects on keratocytes have been observed during keratoconus treatment;[7] and upon testing on rabbit sclera *in vivo*, "serious side-effects were found in the entire posterior globe with almost complete loss of the photoreceptors, the outer nuclear layer and the retinal pigment epithelium (RPE)."[27]

Our present study examines alternative photoactivated systems that maintain the advantages of temporal and spatial control achieved with UV-A/riboflavin. We examine several systems to test for photoactivated strengthening of tissue. The results demonstrate a means to avoid the potential toxicity of UV light by using a visible light activated system of Eosin Y (EY) and triethanolamine (TEOA). This visible light system combines a strong record of biocompatibility with crosslinking ability under irradiation doses that are clinically relevant (conforming to ANSI safety standards).
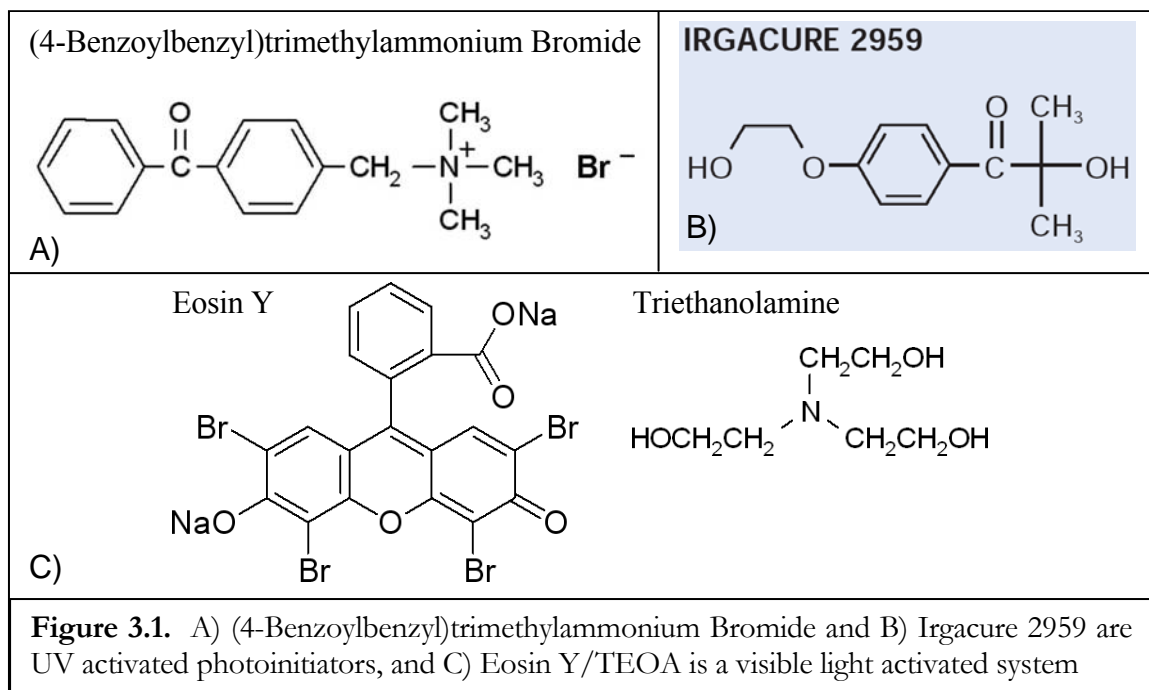
3.2 Photoinitiator Systems

Photoactivated systems rely on light and a photosensitizer—a molecule that is able to generate a radical through the absorption of light. Such systems have been extensively developed for use in coatings and adhesives, and in tissue-engineering applications (Chapter 4). The wavelength of light acceptable in the application guides the selection of the appropriate photosensitizer system. In addition, water solubility, lipophilicity, and cytotoxicity are considered in biological systems.

During the course of this research, three photoinitiator systems have been used (Figure 3.1): two UV photoactivated systems were used for proof of concept. For convenience and solubility in water, preliminary experiments used (4-benzoylbenzyl)trimethylammonium bromide (Figure 3.1a). The demonstration of oxygen inhibition of PEGDM polymerization within the tissue in Chapter 4 uses this initiator. To avoid cytotoxicity, we next examined Irgacure 2959 (I2959, Figure 3.1b), which showed low toxicity over a range of mammalian cell lines relative to other UV-photoinitiators, including Irgacure 184, Irgacure 907, Irgacure 651, CQ/4-N,N-dimethylaminobenzoate, and CQ/Triethanolamine.[28, 29] I2959 is used to demonstrate spatial control of photoactivated crosslinking in this chapter, and to demonstrate strengthening with and without creation of an integrated polymer network in the tissue. Moving toward our goal of eliminating the potential cytotoxic effects of UV light, we devoted the greatest effort to an initiator system for use with visible light, EY with TEOA (Figure 3.1c), which has a well-established track record of biocompatibility in a range of applications (Table 3.1) and has gained FDA approval for use in the human body in the lung sealant FocalSeal® (Genzyme Biosurgical, Cambridge, MA).

EY is a water-soluble xanthene dye and is a common stain for collagen, the main component of the cornea and sclera. EY's absorption peak at 514 nm allows efficient activation with visible light. Upon irradiation, it becomes excited to the triplet state and undergoes electron transfer with TEOA, generating radicals. The combined characteristics of low-toxicity light (green light) and low-toxicity initiator (EY/TEOA) were incorporated in the design of treatment protocols for the majority of *in vitro*, and all of the *in vivo* studies. We use this system to illustrate temporal control of crosslinking in this chapter, to

demonstrate stabilization of eye shape using integrated polymer networks created *in vivo* in Chapter 4, and it is the system used for development toward a treatment of degenerative myopia (Chapter 5) and treatment of keratoconus (Chapter 6).

Figure 3.1. A) (4-Benzoylbenzyl)trimethylammonium Bromide and B) Irgacure 2959 are UV activated photoinitiators, and C) Eosin Y/TEOA is a visible light activated system

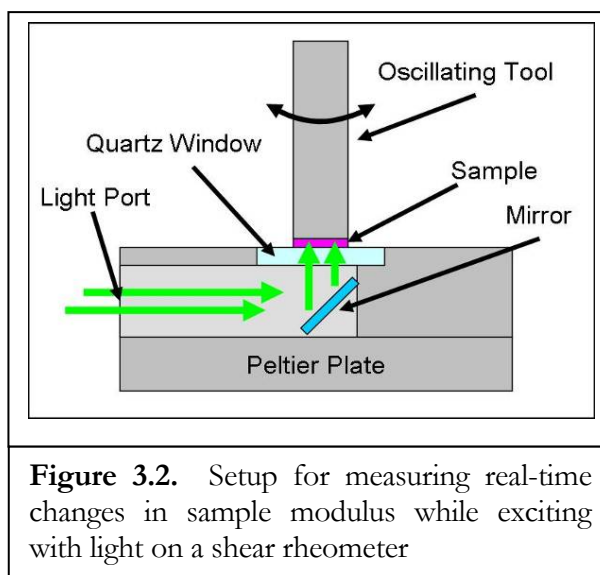| Authors	Application
Nakayama et al.[15]	Hemostasis of Liver Tissue
Orban et al[16]	Cardiovascular Applications
Cruise et. al., Pathak et al., Desmangles et al.[17-19]	Islet Cell Encapsulation / Microencapsulation
Elisseeff et al.[21]	Transdermal Polymerization
Luman et al. Carnahan et al.[22, 23]	Close Linear Corneal Incisions, Secure Lasik flaps
Alleyne et al.[24]	Dural Sealant in Canine Craniotomy (FocalSeal)
West et al.[25, 26]	Thrombosis Inhibition
Table 3.1. Literature Demonstrating Biocompatibility of Eosin Y	

3.3 Temporal and Spatial Control of Treatments

The following *in vitro* experiments illustrate the ability to control the degree of crosslinking using the duration of irradiation, and to achieve spatial control of photoactivated treatments. Collagen gels are used in lieu of cornea or sclera specimens to establish the relationship between irradiation time and extent of crosslinking. Irradiation of porcine sclera through a mask is used to demonstrate spatially resolved activation.

3.3.1 Temporal Control of Treatments

Methods: We have built custom photorheology equipment that allows us to record changes in mechanical properties of specimens during irradiation. Using this, we record the modulus of collagen gels with time before, during, and after irradiation.
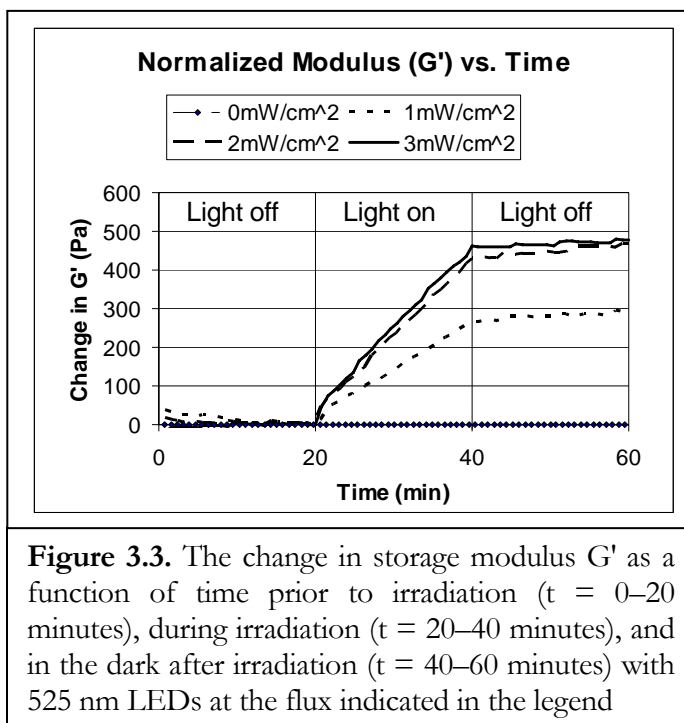
For these experiments, 8-mm-diameter circular sections of 1-mm-thick slabs of 20% gelatin with 0.0289 mM Eosin Y and 90 mM TEOA were mounted on the center of the shear rheometer (AR1000, TA Instruments) modified to allow measurement of light-induced changes (Figure 3.2). The sample was subjected to oscillatory shear with a stress amplitude of 30 Pa and frequency of 0.3 rad/sec, at which the initial storage modulus is approximately 3000 Pa. The dynamic moduli were recorded every 48 seconds for 20 minutes prior to irradiation, during 20 minutes of irradiation, and then monitored for 20 minutes while in the dark (Figure 3.3). Light emitting diodes (LEDs) at 525 ± 16 nm were used to give an irradiance at the sample of 1–3 mW/cm^2.

Figure 3.2. Setup for measuring real-time changes in sample modulus while exciting with light on a shear rheometer

Results: Control samples that receive no light (0 mW/cm^2) do not show any increase in modulus throughout the experiment (Figure 3.3). The change in modulus increases approximately linearly with time at each of the three flux levels examined (1, 2, and 3 mW/cm^2). Further, the increase in modulus does not continue after cessation of irradiation. Therefore, the degree of crosslinking can be controlled using the duration of light exposure. Note that the modulus change may asymptotically approach a maximum rate, and increasing the light intensity beyond a certain value (~3 mW/cm^2) will simply deposit excess energy in the system without increasing the rate. Also note that 5 minutes of irradiation is used in the *in vitro* and *in vivo* experiments described in Chapters 5 & 6. The storage modulus of the model gel increases approximately 5% after 5 minutes of irradiation with a flux in the saturated regime (3 mW/cm^2). Because the increase in modulus is controlled by factors (light intensity and exposure time) that can be easily controlled in the clinic, a treatment can be modified to suit an individual patient. Also, the ability to deliver

the drug to the proper location and then activate it with light will ensure that the proper area is treated.

Photorheological monitoring of crosslinking in collagen gels takes advantage of relatively simple techniques that can be used to screen the effects of light intensity, wavelength, EY concentration, TEOA concentration, and the interactions of these parameters without the use of animals. Future drug optimization experiments requiring animals can then be more intelligently designed based on these test results.

Normalized Modulus (G') vs. Time

Figure 3.3. The change in storage modulus G' as a function of time prior to irradiation (t = 0–20 minutes), during irradiation (t = 20–40 minutes), and in the dark after irradiation (t = 40–60 minutes) with 525 nm LEDs at the flux indicated in the legend
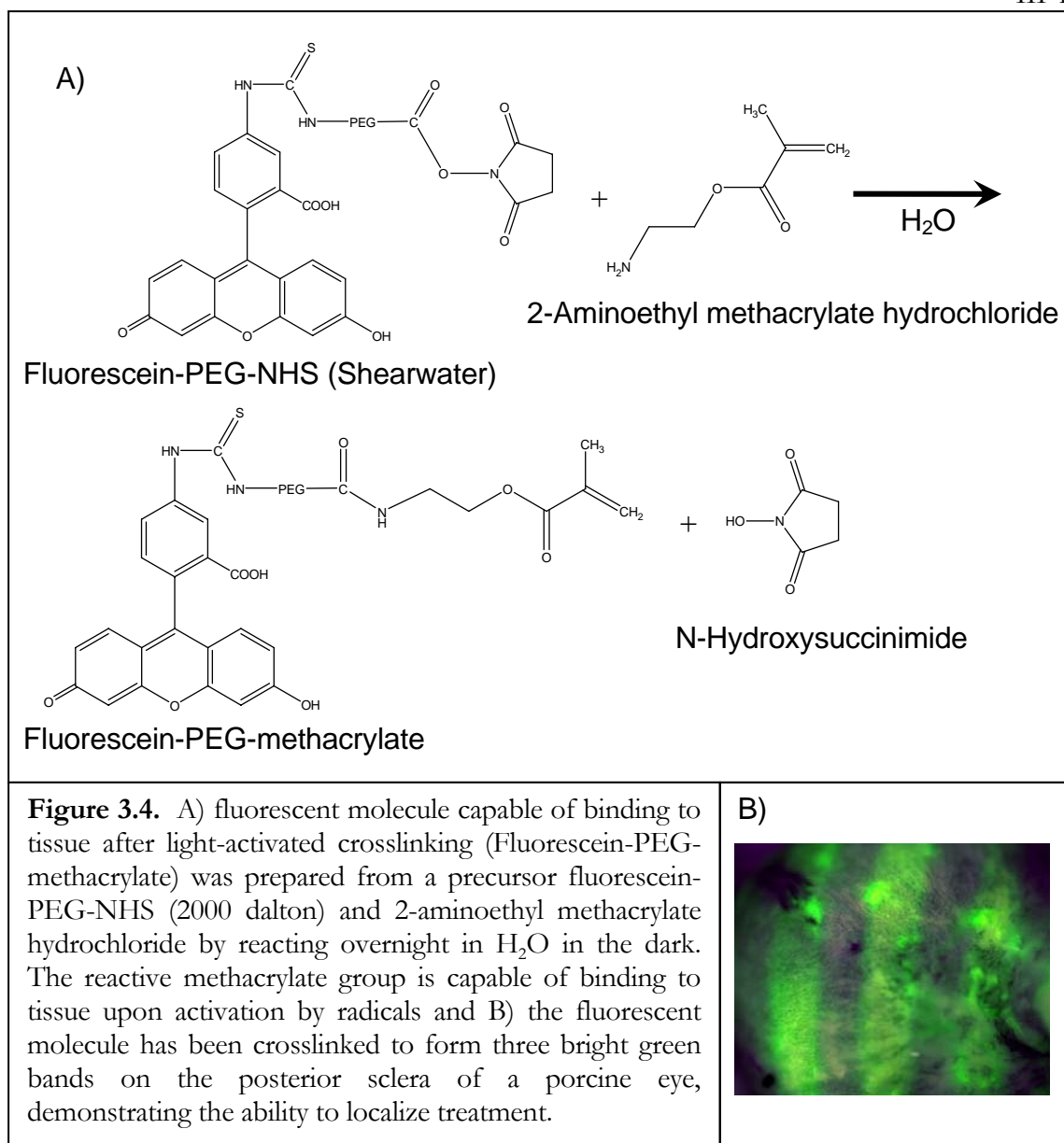
3.3.2 Spatial Control of Treatments

Because the photoinitiator system is only activated upon irradiation with light, it should be possible to selectively activate regions of interest within the tissue. Clinically, this means that drug may be applied to a broad area, and then activated precisely where needed. In

order to determine where treatments are activated, Dr. C.J. Yu synthesized a Fluorescein-PEG-methacrylate (Fluor-PEGM) molecule that is fluorescent and capable of coupling to tissue upon reaction with radicals generated by the photoinitiator (Figure 3.4a). A porcine eye was immersed in a treatment solution (Fluor-PEGM—fluorescent *&* Irgacure 2959—which does not have visible fluorescence) for 5 minutes, then the surface was wiped clean of excess material. A mask was used during irradiation so that only 3 slits of light fell on the posterior sclera. The eye was rinsed in DPBS for 48 hours to allow free Fluor-PEGM to diffuse out of the tissue, and then examined under a black light to visualize fluorescence. Three fluorescent bands were evident (Figure 3.4b). The location of the three fluorescent bands that persist on the sclera correspond to the irradiated regions, indicating activation of the photoinitiator and crosslinking of Fluor-PEGM (Figure 3.4b). The dark bands coincide with areas that did not receive light through the mask.

Treatment of degenerative myopia will likely involve an injection behind the eye, where solution may diffuse into periorbital fat and neighboring muscles. Activation of crosslinking only where light is directed (i.e., onto the sclera) will protect these other tissues. Strengthening of cornea and sclera can also be directed selectively to areas of thinned or weakened tissue without crosslinking healthy areas. Thus, the combined advantages of temporal and spatial control provided by photoinitiator systems increase the ability to tailor treatments to individual patients.

Figure 3.4. A) fluorescent molecule capable of binding to tissue after light-activated crosslinking (Fluorescein-PEG-methacrylate) was prepared from a precursor fluorescein-PEG-NHS (2000 dalton) and 2-aminoethyl methacrylate hydrochloride by reacting overnight in H_2O in the dark. The reactive methacrylate group is capable of binding to tissue upon activation by radicals and B) the fluorescent molecule has been crosslinked to form three bright green bands on the posterior sclera of a porcine eye, demonstrating the ability to localize treatment.

3.4 Light Safety and Clinical Relevance

We hypothesized that visible-light irradiation would facilitate activation of photoinitiator systems using safe levels of irradiation within the cornea and sclera. In view of the experimental results, we compare the irradiation dose that is used above (525 ± 16 nm LEDs, and 6–8 mW/cm^2 at the plane of the tissue) and is used for eye stabilization in

Chapters 5 and 6 to existing standards for safe exposure. The American National

Standards Institute (ANSI) provides the American National Standard for Safe Use of

Lasers[30], and although we are using an LED light source instead of lasers, these standards

provide a guideline for the safe irradiation of the eye. Because of reduced photochemical

hazards at longer wavelengths, the maximum permissible exposure (MPE) of the retina to

green light (525 ± 16 nm) is approximately 30 times greater than the MPE for blue light

(400 nm). We use the MPE for blue light (2.7 J/cm^2) to make a conservative estimate for

irradiation safety. The safety thresholds for clinical treatment of keratoconus are more

stringent than those for degenerative myopia due to the potential exposure of the retina to

the treatment irradiation.

For keratoconus treatment, light directed onto the cornea is transmitted through the cornea,

lens, and vitreous and to the retina with minimal loss. Using the MPE for retinal irradiance

(E_R), we can calculate the maximum permissible source radiance (L_S):

$$L_S = \frac{4 \cdot E_R \cdot f^2}{\pi \cdot \tau \cdot d_P^2}, \; [31]$$

where τ is the transmission through the ocular media (conservatively taken to be 100%), f is

the focal length of the eye (1.7 cm), and d_P is the diameter of the pupil (0.7 cm). This gives

L_S of 20 J/(cm^{2}sr). Calculating the exposure at the cornea can be done using the geometry

of the light source, which can be taken as 1 cm in diameter (D_S) a distance 1 cm from the

cornea (r). The irradiance at the cornea is:

$$E_C = L_S \cdot \frac{\pi \cdot D_S^2}{4 \cdot r^2} = 15.7 \text{ J/cm}^2.$$

For a 300 second exposure, this would correspond to a maximum permissible irradiation of 52 mW/cm^2, which is 6.5 times greater than the irradiation (8 mW/cm^2) used in the *in vitro* keratoconus studies in Chapter 6.

For treatment of degenerative myopia, light delivered from the outside of the eye must pass through the sclera and the choroid before reaching the retina. To obtain conservative safety criteria, calculations here are based upon the minimum thickness and minimum absorption coefficients of the sclera and choroid, neglecting scattering in the sclera and choroid. On this basis, less than 5 % of light incident on the sclera will irradiate the retina (Table 3.2). The MPE for retina remains the same as above (2.7 J/cm^2). Although ANSI does not provide an MPE value for the sclera, exposure of the skin to visible light of duration > 10 seconds should not exceed 200 mW/cm^2. Based on these limits, the irradiation (6–8 mW/cm^2) used in studies on degenerative myopia (Chapter 5) with visible light falls well below the safety limits (by a factor of 25, Figure 3.5).
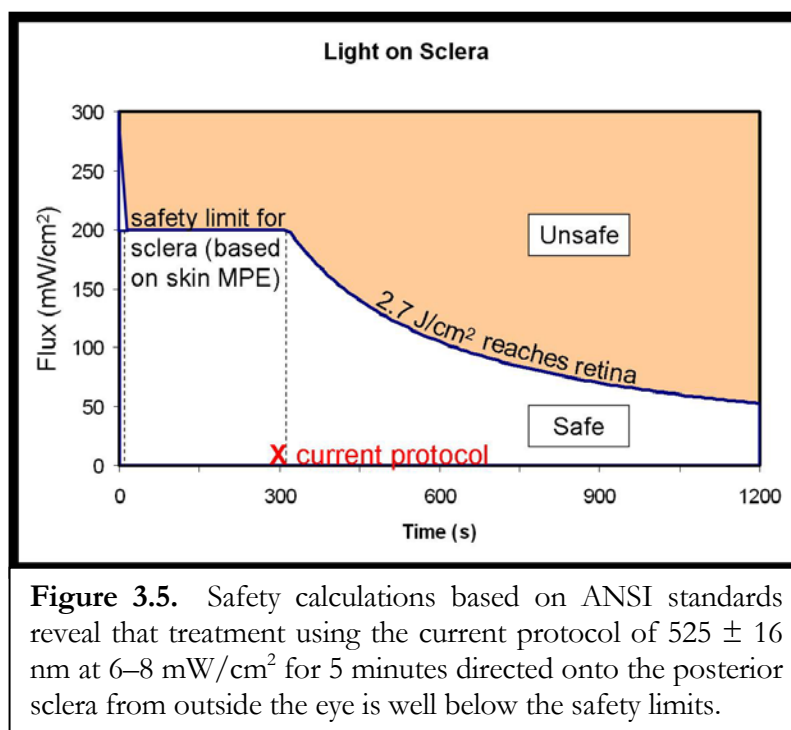
Tissue	Absorption Coefficient, μ (mm^{-1})	Thickness, l (mm)	Transmittance $I/I_{incident} = e^{-\mu l}$
Choroid	15[32]	0.2	0.05
Sclera	0.39 (for 500 nm)[33]	0.39[34]	0.86

Table 3.2 Calculation of Light Absorbed by the Choroid and Sclera

Calculations yield margins of safety with factors of at least 6.5 and 25 for treatment of keratoconus and degenerative myopia, respectively. The safety of this irradiation on rabbit and guinea pig sclera has been verified during *in vivo* biocompatibility studies (Chapter 5).

In relation to clinical application, considerations beyond safety may motivate further reduction of the irradiation dose. The MPE values from ANSI are below known hazardous levels for creation of retinal lesions. Thus, the calculations above indicate that the irradiation used should not damage any ocular tissues; it may still be uncomfortable to view or cause perturbed color perception for a period of time after treatment. Further reduction in intensity may increase patient comfort.

The key factors that led to the decision to use EY/TEOA for development of a clinically relevant treatment in Chapters 5 and 6 are: 1) efficacy with irradiation that is considered safe with respect to ANSI standards, 2) previously demonstrated biocompatibility of EY/TEOA, and 3) temporal and spatial control (like other photoinitiator systems).

Figure 3.5. Safety calculations based on ANSI standards reveal that treatment using the current protocol of 525 ± 16 nm at 6–8 mW/cm^2 for 5 minutes directed onto the posterior sclera from outside the eye is well below the safety limits.

BIBLIOGRAPHY

1. Spoerl, E., Wollensak, G., Dittert, D.D., Seiler, T. Thermomechanical behavior of collagen-cross-linked porcine cornea. *Ophthalmologica* **218**, 136-140 (2004).

2. Spoerl, E., Wollensak, G., Seiler, T. Increased resistance of crosslinked cornea against enzymatic digestion. *Current Eye Research* **29**, 35-40 (2004).

3. Sporl, E., Genth, U., Schmalfuss, K., Seiler, T. Thermo-mechanical behavior of the cornea. *Klinische Monatsblatter Fur Augenheilkunde* **208**, 112-116 (1996).

4. Sporl, E., Genth, U., Schmalfuss, K., Seiler, T. Thermomechanical behavior of the cornea. *German Journal Of Ophthalmology* **5**, 322-327 (1997).

5. Wollensak, G. Crosslinking treatment of progressive keratoconus: new hope. *Current Opinion In Ophthalmology* **17**, 356-360 (2006).

6. Wollensak, G., Aurich, H., Pham, D.T., Wirbelauer, C. Hydration behavior of porcine cornea crosslinked with riboflavin and ultraviolet A. *Journal of Cataract and Refractive Surgery* **33**, 516-521 (2007).

7. Wollensak, G., Spoerl, E., Reber, F., Seiler, T. Keratocyte cytotoxicity of riboflavin/UVA-treatment in vitro. *Eye* **18**, 718-722 (2004).

8. Wollensak, G., Spoerl, E., Seiler, T. Stress-strain measurements of human and porcine corneas after riboflavin-ultraviolet-A-induced cross-linking. *Journal Of Cataract And Refractive Surgery* **29**, 1780-1785 (2003).

9. Wollensak, G., Spoerl, E., Seiler, T. Riboflavin/ultraviolet-A-induced collagen crosslinking for the treatment of keratoconus. *American Journal Of Ophthalmology* **135**, 620-627 (2003).

10. Wollensak, G., Spoerl, E., Wilsch, M., Seiler, T. Endothelial cell damage after riboflavin-ultraviolet-A treatment in the rabbit. *Journal Of Cataract And Refractive Surgery* **29**, 1786-1790 (2003).

11. Wollensak, G., Spoerl, E., Wilsch, M., Seiler, T. Keratocyte apoptosis after corneal collagen cross-linking using riboflavin/UVA treatment. *Cornea* **23**, 43-49 (2004).

12. Wollensak, G., Sporl, E., Reber, F., Pillunat, L., Funk, R. Corneal endothelial cytotoxicity of riboflavin/UVA treatment in vitro. *Ophthalmic Research* **35**, 324-328 (2003).

13. Wollensak, G., Sporl, E., Seiler, T. Treatment of keratoconus by collagen cross linking. *Ophthalmologe* **100**, 44-49 (2003).

14. Wollensak, G., Wilsch, M., Spoerl, E., Seiler, T. Collagen fiber diameter in the rabbit cornea after collagen crosslinking by riboflavin/UVA. *Cornea* **23**, 503-507 (2004).

15. Nakayama, Y., Kameo, T., Ohtaka, A., Hirano, Y. Enhancement of visible light-induced gelation of photocurable gelatin by addition of polymeric amine. *Journal of Photochemistry and Photobiology a-Chemistry* **177**, 205-211 (2006).

16. Orban, J.M., Faucher, K.M., Dluhy, R.A., Chaikof, E.L. Cytomimetic biomaterials. 4. In-situ photopolymerization of phospholipids on an alkylated surface. *Macromolecules* **33**, 4205-4212 (2000).

17. Cruise, G.M., Hegre, O.D., Scharp, D.S., Hubbell, J.A. A sensitivity study of the key parameters in the interfacial photopolymerization of poly(ethylene glycol) diacrylate upon porcine islets. *Biotechnology and Bioengineering* **57**, 655-665 (1998).

18. Pathak, C.P., Sawhney, A.S., Hubbell, J.A. Rapid Photopolymerization of Immunoprotective Gels in Contact with Cells and Tissue. *Journal of the American Chemical Society* **114**, 8311-8312 (1992).

19. Desmangles, A.I., Jordan, O., Marquis-Weible, F. Interfacial photopolymerization of beta-cell clusters: Approaches to reduce coating thickness using ionic and lipophilic dyes. *Biotechnology and Bioengineering* **72**, 634-641 (2001).

20. Wollensak, G., Spoerl, E. Collagen crosslinking of human and porcine sclera. *Journal Of Cataract And Refractive Surgery* **30**, 689-695 (2004).

21. Elisseeff, J., Anseth, K., Sims, D., McIntosh, W., Randolph, M., Langer, R. Transdermal photopolymerization for minimally invasive implantation. *Proc. Natl. Acad. Sci. USA* **96**, 3104-3107 (1999).

22. Carnahan, M.A., Middleton, C., Kim, J., Kim, T., Grinstaff, M.W. Hybrid dendritic-linear polyester-ethers for in situ photopolymerization. *Journal of the American Chemical Society* **124**, 5291-5293 (2002).

23. Luman, N.R., Kim, T., Grinstaff, M.W. Dendritic polymers composed of glycerol and succinic acid: Synthetic methodologies and medical applications. *Pure and Applied Chemistry* **76**, 1375-1385 (2004).

24. Alleyne, C.J.J., Cawley, C.M., Barrow, D.L., Poff, B.C., Powell, M.D., Sawhney, A.S., Dillehay, D.L. Efficacy and biocompatibility of a photopolyrnerized, synthetic, absorbable hydrogel as a dural sealant in a canine craniotomy model. *Journal of Neurosurgery* **88**, 308-313 (1998).

25. West, J.L., Hubbell, J.A. Separation of the arterial wall from blood contact using hydrogel barriers reduces intimal thickening after balloon injury in the

rat: The roles of medial and luminal factors in arterial healing. *Proclomations of the National Academy of Science* **93**, 13188-13193 (1996).

26. Hill-West, J.L., Chowdhury, S.M., Slepianu, M.J., Hubbell, J.A. Inhibition of thrombosis and intimal thickening by in situ photopolymerization of thin hydrogel barriers. *Proclomations of the National Academy of Science* **91**, 5967-5971 (1994).

27. Wollensak, G., Iomdina, E., Dittert, D.D., Salamatina, O., Stoltenburg, G. Cross-linking of scleral collagen in the rabbit using riboflavin and UVA. *Acta Ophthalmologica Scandinavica* **83**, 477-482 (2005).

28. Bryant, S.J., Nuttelman, C.R., Anseth, K.S. Cytocompatibility of UV and visible light photoinitiating systems on cultured NIH/3T3 fibroblasts in vitro. *Journal Of Biomaterials Science-Polymer Edition* **11**, 439-457 (2000).

29. Williams, C.G., Malik, A.N., Kim, T.K., Manson, P.N., Elisseeff, J.H. Variable cytocompatibility of six cell lines with photoinitiators used for polymerizing hydrogels and cell encapsulation. *Biomaterials* **26**, 1211-1218 (2005).

30. American National Standards Institute. *American National Standard for Safe Use of Lasers.* (Laser Institute of America, Orlando, FL, 2000).

31. [Anon]. Guidelines on limits of exposure to broad-band incoherent optical radiation (0.38 to 3 mu M). *Health Physics* **73**, 539-554 (1997).

32. Hammer, M., Roggan, A., Schweitzer, D., Muller, G. Optical-Properties of Ocular Fundus Tissues - an in-Vitro Study Using the Double-Integrating-Sphere Technique and Inverse Monte-Carlo Simulation. *Physics in Medicine and Biology* **40**, 963-978 (1995).

33.   Nemati, B., Rylander, H.G., Welch, A.J. Optical properties of conjunctiva, sclera, and the ciliary body and their consequences for transscleral cyclophotocoagulation. *Applied Optics* **35**, 3321-3327 (1996).

34.   Olsen, T.W., Aaberg, S.Y., Geroski, D.H., Edelhauser, H.F. Human sclera: Thickness and surface area. *American Journal of Ophthalmology* **125**, 237-241 (1998).